J Membrane Biol (2007) 220:53–67
DOI 10.1007/s00232-007-9074-4

Unrestricted Diffusion of Exogenous and Endogenous PIP_2 in Baby Hamster Kidney and Chinese Hamster Ovary Cell Plasmalemma

Alp Yaradanakul · Donald W. Hilgemann

Received: 7 April 2007 / Accepted: 26 September 2007 / Published online: 16 November 2007

Abstract We used two approaches to characterize the lateral mobility of phosphatidylinositol 4,5-bisphosphate (PIP_2) in the plasmalemma of baby hamster kidney and Chinese hamster ovary fibroblasts. First, nitrobenzoxadiazole-labeled C6-phosphatidylcholine and C16-PIP_2 were incorporated into plasma membrane "lawns" ($\sim 20 \times 30$ μm) from these cells and into the outer monolayer of intact cells. Diffusion coefficients determined by fluorescence recovery after photobleaching were similar for the two lipids and were higher in lawns, ~ 0.3 $\mu m^2/s$, than on the cell surface, ~ 0.1 $\mu m^2/s$. For membrane lawns, the fractional recoveries (75–90%) were close to those expected from the fraction of total membrane bleached, and labeling by the probes was several times greater than for intact cells. Second, we analyzed cells expressing M1 muscarinic receptors and green fluorescent protein fused with PIP_2-binding pleckstrin-homology domains, Tubby domains or diacylglycerol (DAG)-binding C1 domains. On-cell gigaseal patches were formed with pipette tips >5 μm in diameter. When the agonist carbachol (0.3 mM) was applied either within or outside of the pipette, lipid signals crossed the pipette barrier rapidly in both directions and membrane blebbing occurred on both membrane sides. Accurate simulations of lipid gradients required diffusion coefficients >1 $\mu m^2/s$. Exogenous DAG also crossed the pipette barrier rapidly. In summary, we found no evidence for restricted diffusion of signaling lipids in these cells. The lower mobility and incorporation of phospholipid at the extracellular leaflet may reflect a more ordered and condensed extracellular monolayer, as expected from previous studies.

Keywords Plasmalemma · Phospholipid diffusion · Fluorescence recovery after photobleaching · Diacylglycerol · Membrane raft · Phosphatidylinositol

A. Yaradanakul (✉) · D. W. Hilgemann
Department of Physiology, University of Texas Southwestern Medical Center at Dallas, Dallas, TX 75390-9040, USA
e-mail: alp.yaradanakul@utsouthwestern.edu

Introduction

The lateral mobilities of phospholipids in cell membranes are of great importance for an understanding of lipid signaling and, especially for the surface membrane of cells, are the subject of multiple controversies (Scherfeld, Kahya & Schwille, 2003). One issue is the extent to which a liquid-ordered phase model (Singer & Nicolson, 1972) must be modified to understand the plasmalemma of real cells and in particular whether phospholipid diffusion is locally constrained by formation of lipid domains and/or protein-defined boundaries. In simple membrane bilayers, diffusion coefficients of many lipophilic probes range 0.4–10 $\mu m^2/s$ (Tocanne, Dupou-Cezanne & Lopez, 1994; Galla et al., 1979; Trauble & Sackmann, 1972). In cell membranes, values for phospholipid probes in the outer cell monolayer tend toward the low range (Pucadyil & Chattopadhyay, 2006; Galla et al., 1979; Trauble & Sackmann, 1972; Schlessinger et al., 1977), with a fraction of probes often appearing immobile (Rimon, Meyerstein & Henis, 1984).

Examples of low mobility are found more often when larger membrane probes are employed (Schlessinger et al., 1976, 1977; Elson et al., 1976), but there are outstanding exceptions. In *Xenopus* oocytes, for example, large fractions of the outer membrane monolayer in the animal pole appear effectively frozen with respect to phospholipid

mobility (Dictus et al., 1984; Tetteroo et al., 1984), and yeast strains are also known to have very low outer monolayer phospholipid mobility (Greenberg & Axelrod, 1993). The reasons for such low mobility are not definitively established. Complex phospholipid interactions (e.g., the influence of cholesterol [Jafri & Keizer, 1995; Golan et al., 1984; Pucadyil & Chattopadhyay, 2006] and formation of "rafts" [Oradd, Westerman & Lindblom, 2005; Siggia, Lippincott-Schwartz & Bekiranov, 2000] do not appear to offer adequate biophysical explanations, nor can massively restricted diffusion be accounted for by the presence of protein (Golan et al., 1984) per se without evoking a "fencing" or corral function of proteins. Sarcoplasmic reticulum, for example, shows rapid phospholipid diffusion in spite of a high protein density (Scandella, Devaux & McConnell, 1972). In summary, there is agreement that the mobile membrane phase of cell membranes can harbor small condensed phases, usually called "rafts," with specialized protein content (Jacobson, Mouritsen & Anderson, 2007; Brown, 2006; Kahya et al., 2004; Chen, Yang & Jacobson, 2004); but the plasticity of such domains (Schuck & Simons, 2004) and the degree of diffusion restriction that might occur within them remain controversial.

On the cytoplasmic side, phosphatidylinositol 4,5-bisphosphate (PIP_2) is an especially important case because it modulates and/or regulates numerous cell processes (van Rheenen et al., 2005; Hilgemann, Feng & Nasuhoglu, 2001). It is a provocative case because PIP_2 accumulates in "light membrane fractions" of sucrose gradients (Liu, Casey & Pike, 1998) that are variously suggested to represent membrane rafts (e.g., Parmryd et al., 2003; Rozelle et al., 2000). Unfortunately, characterization of lipid diffusion in the cytoplasmic monolayer faces many complexities that are not easily addressed (Rimon et al., 1984). In some cell types, notably chromaffin cells (Milosevic et al., 2005), but not all cells (Raucher et al., 2000), PIP_2 appears to exist partially in submicron clusters when imaged with green fluorescent protein (GFP)-coupled pleckstrin homology (PH) domains. These local accumulations of PIP_2 appear to represent real concentration gradients, generated by complex lipid–lipid and lipid–protein interactions, since fluorescent lipophilic dyes do not coaccumulate with the PIP_2 probes (Milosevic et al., 2005). By very similar criteria, a distinct accumulation of PH-GFP domains in membrane ruffles (Tall, Spector, Pentyala) was found to reflect local membrane folding patterns rather than bona fide PIP_2 gradients (van Rheenen & Jalink, 2002).

It is a further problem of great physiological importance to define how, and if, local lipid concentration gradients are generated by localized lipid metabolism. One model is that lateral diffusion of phospholipids is restricted by proteins that form "corrals" (or fences). Tight junctions of epithelial cells evidently define a fence for the inner monolayer of epithelial cells (van Meer & Simons, 1986), phagosomes develop a barrier of unknown nature to lateral lipid diffusion across the invagination boundary before their contents are pinched off (Botelho et al., 2000), the membrane cytoskeleton meshwork is proposed to restrict diffusion on both membrane sides (Kusumi et al., 2005; Dietrich et al., 2002) and present models of endocytosis (Di & DeCamilli, 2006; Kirchhausen et al., 2005) appear to require restrictions of phosphoinositide diffusion out of budding vesicles.

In this context, lipid-metabolizing enzymes of all kinds are known to be localized to specific areas of cell membranes and in complexes with other membrane-associated proteins (Bunce, Gonzales & Anderson, 2006; Santarius, Lee & Anderson, 2006; Ling et al., 2006; Wang et al., 2004; Rhee, 2001; Jenkins & Frohman, 2005). The obvious interpretation of this organization is that local lipid signals are generated within or next to such complexes. As might be predicted, it was recently proposed that highly local PIP_2 signals can be generated in cardiac atrial myocytes in response to activating specific receptors, such that specific receptors couple to specific potassium channel types via local depletion of PIP_2 (Cho et al., 2005a, 2005b). Using a fluorescence recovery after photobleaching (FRAP) technique, it was shown that fluorescent PIP_2, introduced into cells by two means, was virtually immobile (Cho et al., 2005a). Impressively, it was determined that other phospholipids diffused nearly as expected for a simple liquid ordered-phase monolayer and that the near immobility of PIP_2 could be disrupted by disruption of the actin cytoskeleton. Speculatively, therefore, PIP_2 might bind to the cytoskeleton, stabilize it and thereby restrict phospholipid diffusion in a positive-feedback fashion. Interestingly, the same approaches did not suggest that PIP_2 diffusion was restricted in other cell types (Cho, Kim & Ho, 2006).

Given the importance of these issues for understanding PIP_2 signaling and the roles of the cytoskeleton in cell signaling, we have attempted to reproduce the results in multiple cell types and to employ independent experimental approaches to test for a restriction of PIP_2 diffusion in the cytoplasmic monolayer. First, we analyze exogenous fluorescent PIP_2 mobility in a plasmalemmal "membrane lawn" model with comparisons to the outer cell surface. Second, we analyze endogenous PIP_2 mobility via PIP_2-binding domains fused with GFP (Raucher et al., 2000) in patch-clamped cells with activation of phospholipase C (PLC)-coupled receptors either within or outside of the patch pipette. Third, we provide simulations of diffusion as a quantitative basis for interpreting the results. In short, we find no evidence for diffusion restrictions that would be required to generate lipid gradients by local lipid kinase, phosphatase and lipase activities.

Methods

Whole-Cell Patch-Clamp and Pipette Perfusion of the Cytoplasm

Patch-clamp and patch-pipette perfusion were carried out as described at 36°C (Hilgemann & Lu, 1998). Briefly, an Axopatch 200B patch clamp was employed for both on-cell and whole-cell recording (Molecular Devices, Sunnyvale, CA). Glass tubing was pulled to yield tip openings of 4–8 μm and slightly polished without cutting. Pipette-perfusion experiments were carried out with gigaseals in the range of 3–10 GΩ. To do so, flexible quartz capillary tubing (109 μm outside diameter, 40 μm inside diameter; Polymicro-Technologies, Phoenix, AZ) was positioned with a one-dimensional hydraulic manipulator in the patch pipette so that the solution outlet was located within 40 μ of the patch membrane. When positive pressure was applied to a 100-μl solution reservoir, solution in the patch pipette tip was effectively exchanged within 10 s.

Cell Culture and Transfection

A baby hamster kidney (BHK) cell line was transfected with pcDNA3.1/hg for the human muscarinic hM1 receptor (Selyanko et al., 2000) and selected with 400 μg/ml of hygromycin B (Sigma, St. Louis, MO; H0654). Cultures were maintained in collagen-coated 6-cm dishes in Dulbecco's modified Eagle medium (DMEM) containing 10% (v/v) fetal bovine serum (FBS), 100 units/ml penicillin-streptomycin at 37°C with 5% CO_2 and 100% humidity. Chinese hamster ovary (CHO) hM1 cells (Selyanko et al., 2000) were maintained in F-12K medium containing the same amount of FBS and penicillin-streptomycin with 300 μg/ml G418. Cells at 50–70% confluence were transfected with PH-GFP or C1-GFP plasmids using Lipofectamine 2000 reagent according to the manufacturer's instructions (Invitrogen, Carlsbad, CA). After 18–24 h, cells were trypsinized and kept in the same DMEM for experimental use. All experiments were conducted 24–36 h after transfection.

Membrane Lawn Preparation

Membrane lawns were prepared from BHK cells grown on coverslips, largely as described (Hussain et al., 1999; Shpetner, Herskovits & Vallee, 1996; Moore & Anderson, 1989). BHK cells were initially grown to 80% confluence and removed from culture dishes by trypsinization. The cells were then plated onto 22 × 40 mm no. 1 coverslips that had been washed with ethanol and dried briefly on a flame. Coverslips were placed into 35-mm tissue culture dishes containing 3 ml cell culture medium with 10% FBS and 100 units/ml penicillin-streptomycin and cultured for 24h to obtain approximately 50% confluence. Coverslips were then transferred into culture dishes containing phosphate-buffered saline diluted by 50% with 2.5 mM $MgCl_2$ for 1.5 h at 4°C. After a brief wash, cells were sonicated in 8 ml of the same solution for 2 s by moving the dish with the 0.5-inch tapered horn held 1 cm above the coverslip at setting 40 (Sonics and Materials Vibra Cell, Newtown, CT). The dishes were rocked gently to remove sheered cells, and the remaining cells were washed with the same buffer solution. Coverslips then contained approximately equal numbers of membrane lawns and undamaged cells. Before experiments, the membrane lawns were washed three times with 2 ml of a high-K solution containing lipid phosphatase inhibitors (10 mM $Na_4P_2O_7$, 60 mM KF, 5 mM ethylenediaminetetraacetic acid [EDTA], 20 mM Na_2HPO_4, 0.02 mM Na_3VO_4).

Fluorescent Labeling of Membranes

1-Oleoyl-2-[6[(7-nitro-2-1,3-benzoxadiazol-4-yl)amino]hexanoyl]-*sn*-glycero-3-phosphocholine (NBD-PC; Avanti Polar Lipids, Birmingham, AL) and D^+-*sn*-1-*O*-[1-[6′-[6-[(7-nitrobenz-2-oxa-1,2,-dazol-4-yl)amino]hexanol]amino]-hexanoyul]-2-*O*-hexadecanolylglyceryl E-myophosphatidylinositol 4,5,-bisphosphate (NBD- PIP_2; Echelon Biosciences Inc., Salt Lake City, UT) were dissolved in ethyl alcohol at a stock concentration of 1 μg/μl. Membrane lawns were labeled by incubation with 2 μM NBD-PC or NBD-PIP_2 in K-saline at 4°C for 30 min. After staining, the coverslips were washed three times with K-saline and kept at 4°C. FRAP was then performed at room temperature (23°C) in K-saline using a large-volume open diamond bath polycarbonate imaging chamber (Warner Instruments, Hamden, CT; RC26G and PH-1) that allowed convenient solution changes.

Imaging, FRAP and Data Analysis

The experiments were performed with a Zeiss (Thornwood, NY) LSM 510 confocal microscope equipped with 25-mW argon-ion laser operating at dual wavelengths, 488 and 514 nm, and a second laser at 543 nm (Lasos LGK 7812 ML3 488/514, LGK 7786-P 543 nm). FRAP was carried out at room temperature of 23°C via rectangular illumination with a variable width. The laser output was attenuated to 1/500 for monitoring the recovery. A Zeiss 63 × 1.40 NA oil immersion lens was used for imaging. A stripe within the membrane lawn or cell was bleached for just long enough

to reduce fluorescence emission by about 50%, and recoveries were recorded by taking just enough images to allow accurate reconstruction of the time courses. Given the lability of NBD fluorescence, we routinely adjusted imaging settings, frequency and experiment durations to insure that photobleaching was negligible in the results for analysis.

As illustrated in "Results," we used Matlab to simulate FRAP results for membrane stripes from the diffusion equation in one dimension:

$$\frac{\partial C(x,t)}{\partial t} = D\,\frac{\partial^2 C(x,t)}{\partial x^2} \tag{1}$$

The Bulirsch-Stoer method was employed with polynomial extrapolation for integration (Press et al., 1986), and the boundary condition was defined as a stripe containing no dye ($C = 0$), bounded by 10 times larger stripes on both sides with a uniform dye concentration ($C = 1$). Experimental results were then analyzed by scaling simulated results to the data and fitting the optimal diffusion coefficient (D). In addition, we determined the best diffusion coefficients via an equation derived empirically (Ellenberg et al., 1997) to describe FRAP data with high precision:

$$C_{stripe(t)} = C_{stripe(final)} \cdot \left\{1 - \left[w^2\left(w^2 + \alpha Dt\right)^{-1}\right]^{1/2}\right\} \tag{2}$$

Here, C_{stripe} is the average concentration of dye in the stripe area, w is the full width of the stripe, D is the diffusion coefficient, t is time and α is an empirically determined coefficient. With $\alpha = 1.78$, we found that this equation described the appropriate discrete simulations of FRAP with high precision.

Results

Disposition of Exogenous Phospholipids in Cells

Cho et al. (2005a) introduced exogenous fluorescent PIP_2 into cardiac myocytes by two means, whole-cell patch-clamp pipettes and a lipid carrier system. In preliminary experiments, therefore, we attempted to perfuse fluorescent phospholipids into cells via large-diameter pipettes with 4- to 8-μm openings, which we use routinely for whole-cell voltage clamping (Hilgemann & Lu, 1998). Our expectation was that phospholipids might adhere to the pipette wall and diffuse preferentially into the cytoplasmic leaflet of the cell membrane, as appears to occur in giant excised patches (Collins & Hilgemann, 1993; Hilgemann & Collins, 1992). As shown in Figure 1 for C16-NBD- PIP_2, that is not the case. Figure 1a shows the typical whole-cell patch clamp of a BHK cell with a quartz capillary perfusion line within the patch pipette. The cell has a gigaseal, and the pipette opening is just 6 μm. For 2 min, 2 μM NBD-PIP_2 was perfused into the cell, and then the cell was again perfused with lipid-free cytoplasmic solution. As shown in Figure 1b, the remaining fluorescence was very diffuse and showed no selective labeling of the surface membrane. The extent to which the NBD fluorescence reflects lipid that is inserted into membranes or bound tightly by proteins is unknown. Similar results were obtained with other fluorescent probes (e.g., FM dyes used for membrane cycling studies [Rizzoli, Richards & Betz, 2003]) and with other cell types, including cardiac myocytes. From these outcomes, we concluded that the FRAP technique could not be employed for our purposes with direct application of exogenous phospholipids to the cytoplasmic side of intact cells.

NBD-PC and NBD-PIP_2 Diffusion on the Surface of Cells

Figure 2 describes our determination of diffusion coefficients for NBD-PC and NBD-PIP_2 on the surface of BHK cells. Figure 2a shows simulations of a FRAP protocol in which a stripe 4 μm wide is bleached in the central region of a rectangular membrane that is 84 μm wide and has a diffusion coefficient of 0.5 $\mu m^2/s$. Simulated curve 1 gives the fluorescence recovery at the middle of the stripe, curve 2 (dashed) gives the average fluorescence of the stripe, curve 3 (solid) gives the best fit of equation 2 to the recovery curve and curve 4 gives the fluorescence at the edge of the rectangle. Note that deviation of the recovery curve from the curve predicted by equation 2 is within the experimental noise of data described subsequently. Also, it is noteworthy that the recovery curve appears to reach an asymptote at about 76% recovery toward the concentration at the edge (curve 4), although with time the concentrations in the entire rectangle will equalize.

Figure 2b and c shows data from single FRAP experiments for NBD-PIP_2 and NBD-PC, respectively. The lipids were applied for 5 min at concentrations of 2 μM, followed by multiple washes, and 2-μm-wide regions were bleached at the edges of cells. Included in both panels are recovery data (curve 1), the best fits of equation 2 (curve 2, dashed) and the best description via discrete simulation (curve 3, solid). Figure 2d gives the average diffusion coefficients, 0.079 and 0.044 $\mu m^2/s$, respectively, for NBD-PIP_2 and NBD-PC. The difference is not significant ($P = 0.09$). Figure 2e gives the percent recovery of fluorescence within 150 s. Recovery is significantly reduced at 150 s from 81% to 71% with PC *vs.* PIP_2. From simulations, it is likely that the recoveries at 150 s do not reflect immobile lipids and

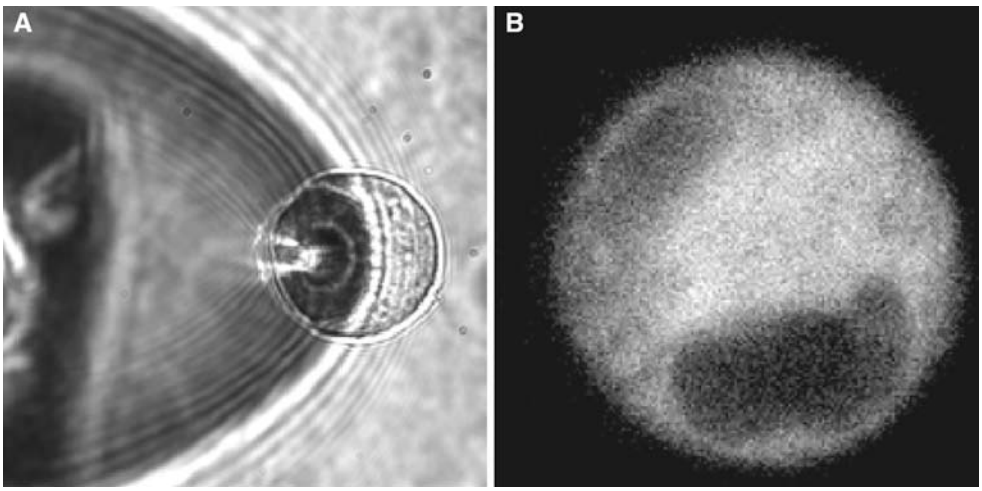

Fig. 1 **(a)** BHK cell in whole-cell voltage clamp with giant patch pipettes (~6 μm diameter opening). A quartz perfusion line with 109 μm outer diameter is used to perfuse solution with 2 μM NBD-PIP_2 toward the pipette orifice and into the cell (*left portion of patch pipette*). This line can be moved toward and away from the cell opening via a hydraulic micromanipulator. **(b)** Typical confocal fluorescence micrograph of a BHK cell that was perfused with NBD-PIP_2 liposomes for 2 min and then with PIP_2-free solution for 2 min. The fluorescent lipids clearly bind throughout the cytoplasm, and surface membrane is not selectively labeled. Results for a number of hydrophobic membrane probes were similar

that the reduced recovery for PC can be explained by a somewhat smaller diffusion coefficient. Since the diffusion coefficients were substantially smaller than expected for simple bilayers, we tested two interventions that might be expected to influence diffusion. First, we treated cells with latrunculin to disrupt the actin cytoskeleton, and changes were not evident. Second, for NBD-PC we confirmed that cholesterol removal by 6 mM β-methylcyclodextran for 15 min increased the diffusion coefficient more than twofold (Pucadyil & Chattopadhyay, 2006; Ilangumaran & Hoessli, 1998).

NBD-PC and NBD-PIP_2 Diffusion in Membrane Lawns

The membrane lawn preparation (Hussain et al., 1999; Shpetner et al., 1996) has the advantage for our purpose of free access to the cytoplasmic side with reasonable maintenance of membrane cytoskeletal structures (Aggeler, Takemura & Werb, 1983; Moore & Anderson, 1989) after removal of cell constituents. Thus, it seems possible, at least, that diffusion restrictions related to the cytoskeleton and other membrane-associated proteins would be intact after sonication. A clear disadvantage is that phospholipids will presumably reach both membrane surfaces and that membrane asymmetry will likely be disrupted. Our expectation, therefore, was that FRAP signals would be complex but might reveal the presence of slow components that could be analyzed and manipulated.

Figure 3 shows typical fluorescence images of the membrane lawns after labeling with either 2 μM NBD-PC (upper images) or 2 μM NBD-PIP_2 (lower images), applied as described in "Methods" and followed by extensive washout. The fluorescence appears mostly homogeneous over the entire lawn dimensions of roughly 20 × 30 μm for both probes. Figure 3b and e shows images of the lawns immediately after photobleaching stripes, and Figure 3c and f show the same lawns after 45 s of recovery. As apparent, recovery was largely complete in this time frame for both lipids. Figure 4 shows FRAP time courses for 4-μm stripes bleached in membrane lawns labeled with NBD-PC and PIP_2. Figure 4b also shows the time course for an 8-μm stripe (dotted line), and dashed lines show the best fits to equation 2. The diffusion coefficients are 0.062 and 0.17 $\mu m^2/s$ for PC and PIP_2, respectively. One concern with narrow bleach stripes is that the bleach may extend beyond the intended border and thereby cause artifactually low diffusion coefficients. However, as evident here, diffusion coefficients determined with wider stripes were not markedly different (0.20 *vs.* 0.17 $\mu m^2/s$). The approximate 75% recoveries of fluorescence in these membrane lawns correspond reasonably to the recovery expected, given the nonexponential nature of recovery pointed out above and the fact that about 15% of the total lawn area is bleached. From further experiments, we determined the average NBD-PC diffusion coefficient in the lawns to be 0.18 ± 0.02 $\mu m^2/s$ ($n = 5$). For NBD-PIP_2 on membrane lawns, an average diffusion coefficient of 0.16 ± 0.06 $\mu m^2/s$ ($n = 20$) was obtained. Figure 5 shows typical Z-scans of fluorescence intensity for a membrane lawn and an intact cell on the same coverslip. The incorporation of NBD-phospholipids on the membrane lawns was almost four times greater than on the intact cell plasma membrane, and possible reasons for this difference will be discussed.

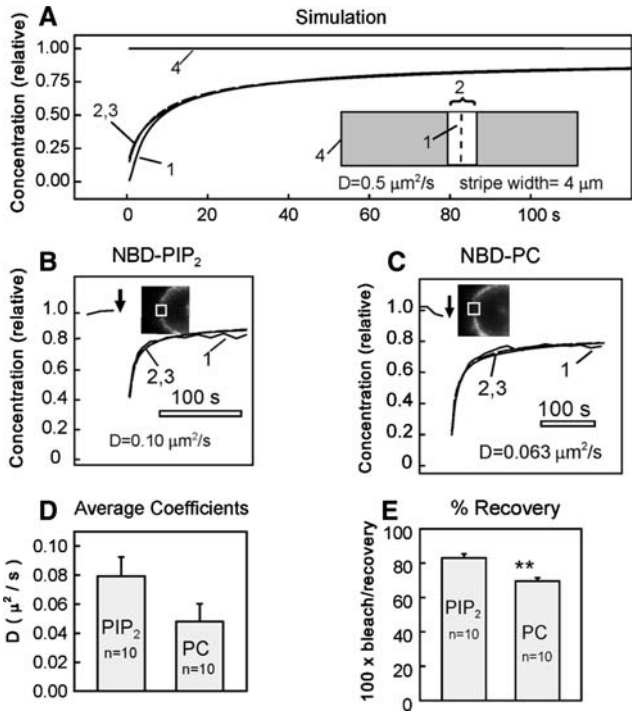

Fig. 2 Time courses of fluorescence recovery in intact BHK cells after bleaching NBD-labeled PIP_2 and PC. **(a)** Simulation of lipid diffusion in a planar sheet assumed to be 44 μm wide. At zero time, the lipid concentration is 0 in a 4-μm stripe in the middle of the sheet and the concentration everywhere else is 1. *Curve 1* depicts the concentration recovery at the center of the stripe, *curve 2* (*dashed*) gives the average concentration in the stripe, *curve 3* (*solid*) gives the prediction of equation 2 described in "Methods" and *curve 4* is the lipid concentration at the far edge of the membrane. Note that the far edge and the stripe do not approach equilibrium in a simple exponential manner, so it appears as if there is an immobile fraction of lipid. **(b, c)** Experimental FRAP data for BHK cells stained with 2 μM NBD-PIP_2 and NBD-PC, respectively. Micrographs show the cell images just after bleaching, where *rectangles* correspond to the bleached area. *Curves 2* (*dashed*) give the best fit to equation 2, and *curves 3* give the equivalent discrete simulations with the best-fit diffusion coefficient. **(d)** Average diffusion coefficients from 10 experiments for each probe. **(e)** Percentage recovery of fluorescence at 150 s for the two probes

PIP_2 Diffusion in Intact Cells

The experiments just described have multiple limitations that will be discussed. To determine mobility of endogenous PIP_2 in the cytoplasmic leaflet, we devised a strategy using the on-cell patch-clamp recording configuration with cells expressing PIP_2-binding domains and hM1 muscarinic receptors. To facilitate imaging, the patch pipette tip was positioned nearly parallel to the microscope stage and the pipettes employed were pulled to have a rather shallow taper to the tip. Our tactic was to exploit the on-cell giant patch configuration in which receptors can be activated within the pipette via rapid intrapipette perfusion of agonist. In this case, the propagation of the lipid signal into membrane outside of the pipette can be monitored. Conversely, agonists can be applied outside of the pipette and penetration of the lipid depletion into the membrane within the giant pipette can be monitored. Both CHO and BHK cells were employed, and results were very similar.

Figure 6a shows a typical image of the PH-GFP domain fluorescence of a CHO cell expressing hM1 receptors before applying agonist (0.3 mM carbachol) into the pipette. The PH domains are located largely at the cell surface, and the membrane is pulled somewhat into the pipette orifice by the gigaohm seal formation (region 1). Upon perfusion of carbachol into the pipette tip, there is a rapid decrease of fluorescence at the membrane within the pipette tip, followed approximately 8 s later by a decrease of PH domain at membrane outside of the pipette (membrane region 2). PH domains from all membranes in the focal plane of the cell translocated eventually into the cytoplasm as PIP_2 was evidently hydrolyzed, and this was followed by a gradual recovery in time. We note an abrupt increase of fluorescence in the signal recorded within the pipette at approximately 33 s. This corresponds to a shift of membrane position in the pipette that is associated with formation of membrane blebs with PLC activation, as described in subsequent figures.

To account for these results in simulations, we find that PIP_2 diffusion coefficients must be larger than determined in membrane lawns. Figure 6c shows a simulation in which it is assumed, as in the Appendix, that PIP_2 is being constantly dephosphorylated and phosphorylated so that total PIP_2 turnover occurs with a time constant of 20 s. With this turnover, the simulated activation of PIP_2 degradation in 10% of the cell membrane leads to cellular PIP_2 depletion with approximately the right delays and time courses when the diffusion coefficient is 0.7 $\mu m^2/s$. We note that if the basal turnover of PIP_2 is assumed to occur more slowly, the depletion signals continue for a longer period of time and are of larger magnitude. In other words, the time course with which these signals come to a steady state is presumably determined by continuous turnover of PIP_2 in the membrane that is not exposed to carbachol.

Figure 7 shows typical results obtained when carbachol was applied to the cell membrane outside the gigasealed on-cell patch pipette. Line scans are shown perpendicular to the patch pipette (vertical line) and directly through the axis of the pipette (horizontal line). The interval between exposures was 3 s. Before agonist exposure, at times t_{0-2}, PH-GFP domains are mostly accumulated on the plasma membrane. Fluorescence of the free cell membrane in the pipette is greater than in the overall cell membrane, presumably as a result of optical aberrations. When carbachol is introduced into the chamber at time t_3, fluorescence of the cell membrane decreases with a time constant of about 3 s (see line scans at t_3 and t_6 and in Fig. 8d). Within the pipette, membrane fluorescence decreases with a delay of

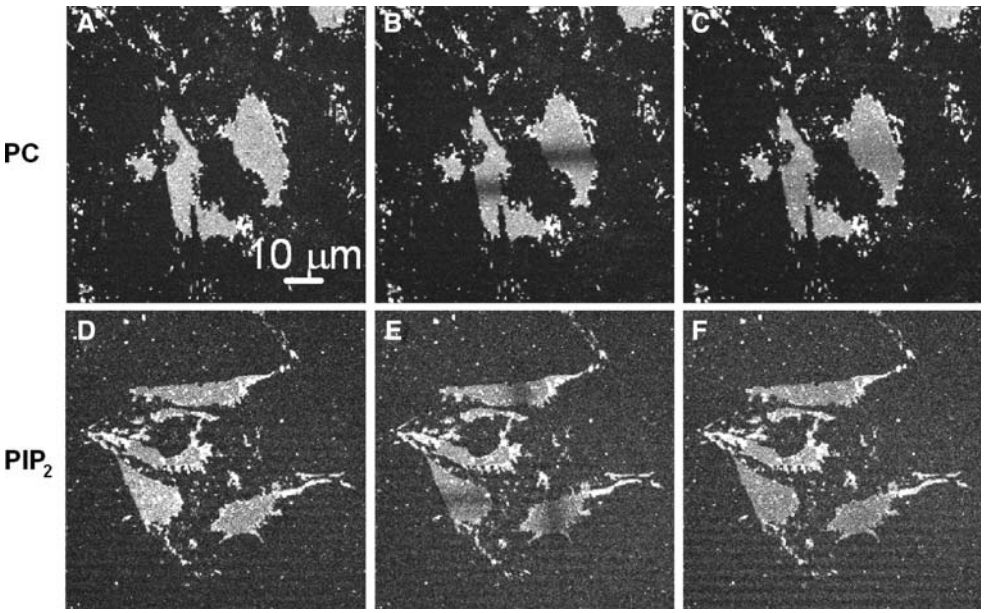

Fig. 3 Typical confocal images from FRAP experiments using BHK membrane lawns stained with 2 μM NBD-PC in **a–c** and 2 μM NBD-PIP_2 in **d–f**. The membranes are incubated in high-K solution with a cocktail of lipid phosphatase inhibitors. The images were taken just before (**a, d**) and just after (**b, e**) bleaching membrane stripes and after 45 s recovery from photobleach (**c, f**). The recovery after photobleach was recorded with 1/500 of the laser intensity used for photobleaching

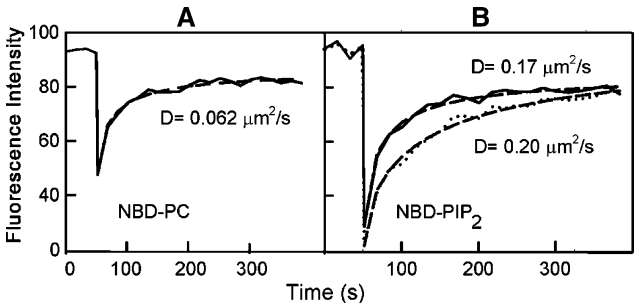

Fig. 4 Fluorescence time courses in typical FRAP experiments using BHK membrane lawns stained with NBD-PC **(a)** and NBD-PIP_2 (**b**). About 15% of the fluorescence is bleached. *Solid lines* are with 4-μm stripes, and *dotted line* illustrates responses for an 8-μm stripe. *Dashed lines* give the best fits of equation 2 to the data, resulting in the diffusion coefficients given in the figure

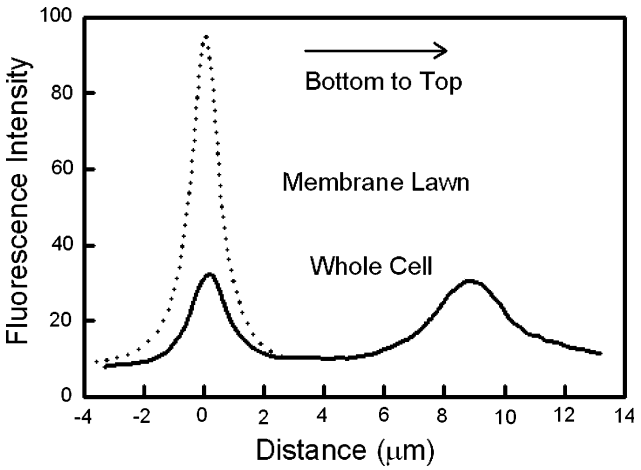

Fig. 5 Z-scans of NBD-PC-labeled whole BHK cell (*solid line*) and BHK membrane lawn (*dashed line*) on the same coverslip. The step size is 0.3 μm with the same solutions and identical microscope setting. Incorporation of NBD-PC is four times greater in the membrane lawn than in the surface of the intact cell

about 5 s. Since the signals throughout the cell membrane exposed to carbachol were similar, we averaged them and present normalized results for the whole cell and the membrane in the patch pipette in the right panel of Figure 7d. The delay between signals is less than 5 s for a diffusion distance of about 6 μ from the edge of the pipette to the free membrane within the pipette. For rough estimation of the diffusion coefficieint, we assume that $D = 0.5\ x^2/\tau$, where x is distance and τ is the apparent time constant. The diffusion coefficient obtained, 3.5 $\mu m^2/s$, is still larger than expected from the pipette application of carbachol, and conclusions from simulations were similar. We used line scans for this analysis at positions where no membrane blebbing was observed.

To test whether IP_3 kinetics significantly affect the PH domain signals, we performed similar experiments with the PIP_2-binding domain of the Tubby protein, a transcription factor that binds with high specificity to PIP_2 but does not bind IP_3 (Santagata et al., 2001; Brown et al., 2007) and that has also been used as a fusion protein to monitor PIP_2 kinetics (Brown et al., 2007). As shown in Figure 8, the introduction of carbachol into the pipette stimulates as expected release of the Tubby domain from the plasma membrane of a BHK cell in gigaseal formation and expressing hM1 receptor. In Figure 8a, fluorescence intensities are shown for four different regions of the cell. Before carbachol exposure, t_{0-1}, the domain is mostly associated with the surface membrane. The horizontal line scan of the image crosses the cell at the edge of the pipette and the far end of the cell in the chamber. The perpendicular line crosses almost through the center line of the cell. When carbachol was introduced into the pipette,

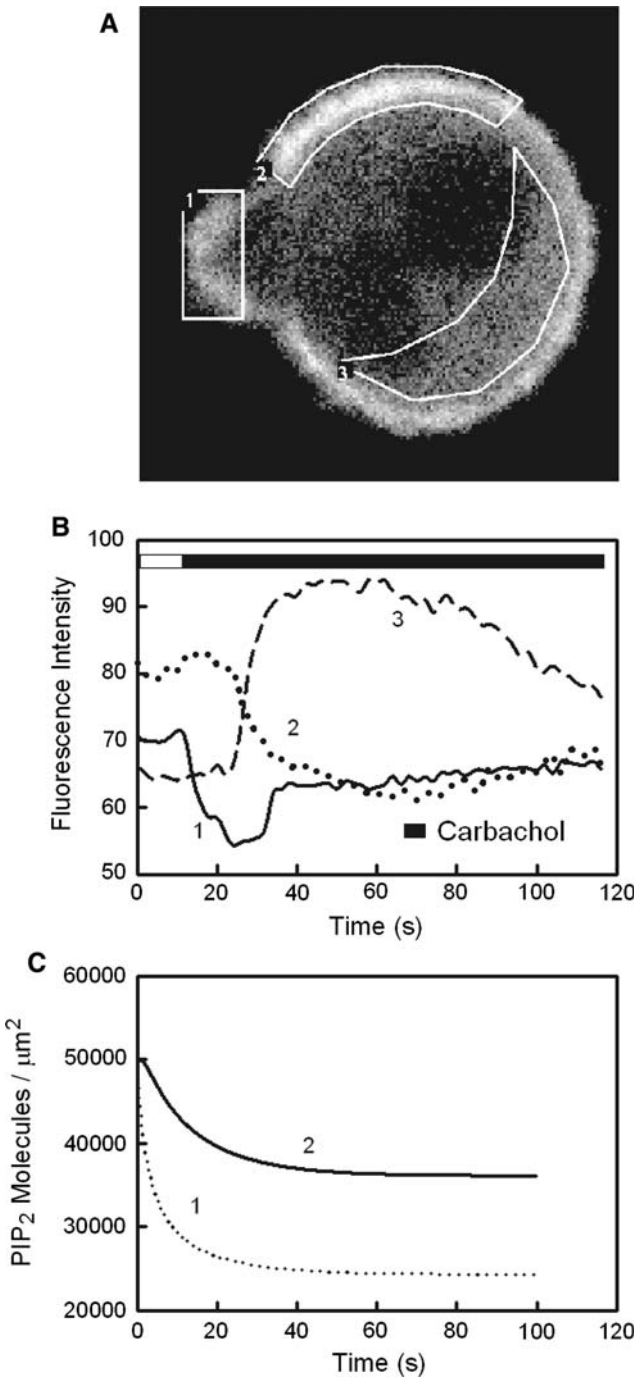

Fig. 6 **(a)** Rapid perfusion of carbachol into a giant on-cell patch pipette with gigaseal (region 1) on a CHO cell overexpressing hM1 muscarinic receptors and GFP-PH domains. **(b)** When the cholinergic agonist carbachol (300 μM) is introduced into the pipette tip at the tenth second, PH domains initially are lost from membrane in voltage clamp. However, the focal depletion spreads to membrane outside the pipette (*region 2*, *dotted line*) within 10 s, and PH domains accumulate in the cytoplasm of the cell (*region 3*, *dashed line*) with a similar time course. The GFP signal at the membrane in the pipette (*solid line*) increases abruptly at about 32 s as a result of membrane blebbing in the pipette tip. **(c)** Simulation of experimental results. See text for details

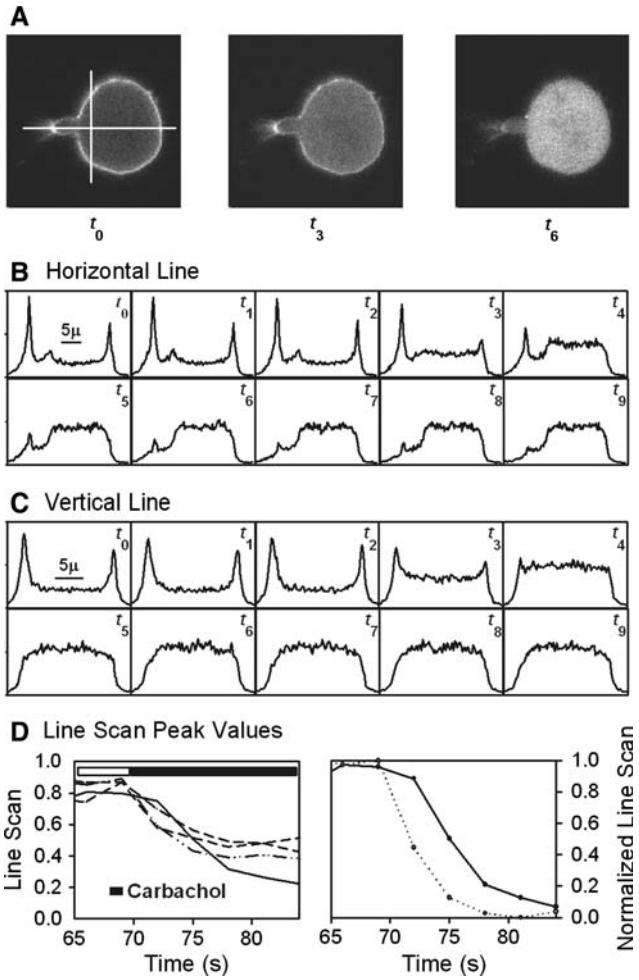

Fig. 7 **(a)** Fluorescence micrographs of PH-GFP domains in BHK cell expressing hM1 receptors with giant patch pipette attached in on-cell configuration. *Images from left to right* are before (t_0), immediately after (t_3) and 10 s after (t_6) carbachol application. *Horizontal and vertical line scans* are shown for these and additional time points at 3 s intervals, namely $t_{0,9,}$ corresponding to 9, 6 and 3 s before carbachol and 0, 3, 6, 9, 12, 15 and 18 s after carbachol application in the bath solution outside of the pipette. **(b)** *Horizontal line scans* for 10 consecutive exposures show the latency in the decrease of the peak membrane fluorescence in the pipette at t_3. **(c)** *Vertical line scans* show simultaneous drop of fluorescence throughout the cell membrane outside of the pipette. **(d)** (*Left*) Comparison of membrane fluorescence signals recorded outside of the pipette (*dashed line*) and within the pipette (*solid line*). (*Right*) Normalized line scans for the average of membrane-associated fluorescence outside of the pipette (*dotted line*) and within the pipette (*solid line*). The time delay of PIP_2 depletion in the pipette is less then 5 s, corresponding to PIP_2 diffusion over approximately 6 μm along the tip of the pipette

fluorescence began to decrease at the near edge at time t_3 followed by the far edge at t_5 and continued to decrease with a time constant of about 5 s, somewhat slower than determined with the PH domains. Presumably, this difference reflects the higher specific affinity of the Tubby domain for PIP_2 as well as the lack of influence of inositol

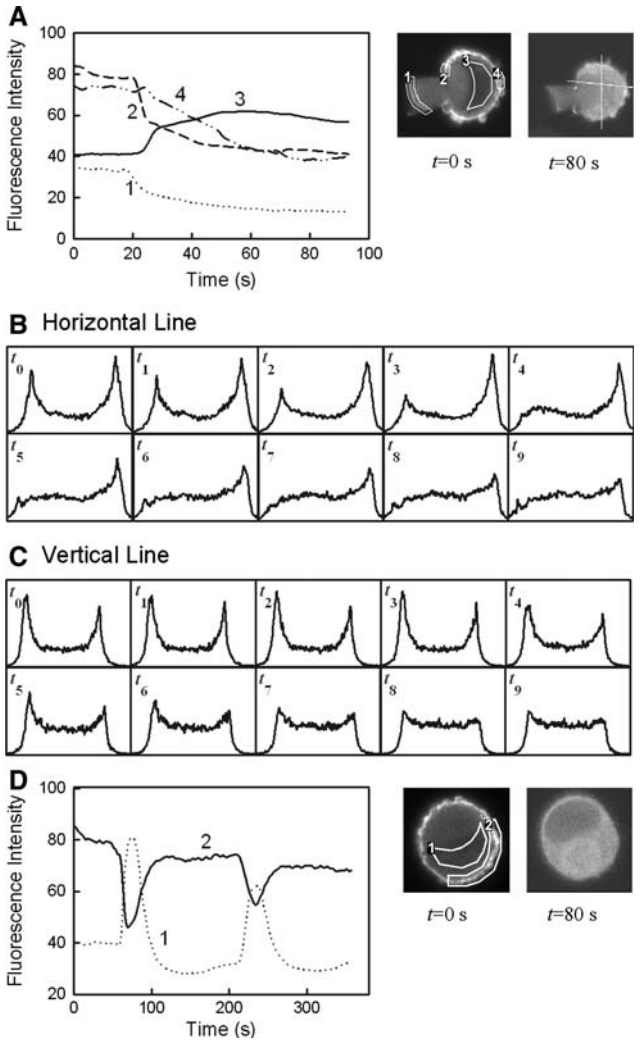

Fig. 8 Florescence signals from Tubby-GFP fusion proteins transiently expressed in BHK cells expressing hM1 receptors. **(a)** Cytoplasmic fluorescence changes upon carbachol perfusion into the pipette tip. Receptor activation in membrane within the pipette releases Tubby domains remotely. **(b)** *Horizontal line scans* for 10 consecutive exposures at 3 s time intervals. The line crosses the pipette edge and the far end of the cell. Membrane fluorescence decreases first at the pipette, followed by a delayed decrease at the other end of the cell. **(c)** A *vertical line* crosses the plasma membrane at similar distances from the pipette, and membrane fluorescence decreases simultaneously at the two membrane crossings. **(d)** An intact cell is exposed to carbachol twice, and optical signals on the plasma membrane and in the cytoplasm mimic results for PH domains

1,4,5-triphosphate (IP_3). The peaks associated with the scans drop at nearly the same rate at opposite ends. Figure 8d shows multiple responses of the Tubby domains that were readily obtained in intact cells from sequential applications of 0.3 mM carbachol for 10 s. From this and similar experiments, our estimates of PIP_2 diffusion coefficients range 1.5–2.5 $\mu m^2/s$.

Finally, we performed equivalent experiments to determine whether gradients of diacylglycerol (DAG)-binding C1-GFP domains might be detected in the same BHK and CHO cell lines stably expressing hM1 receptors. In this case, a loss of cytoplasmic fluorescence occurs when DAG in the surface membrane increases as the C1-GFP domains move to the plasma membrane. As shown in Figure 9 for a BHK cell, strong C1 domain signals could be evoked multiple times by applying and removing carbachol (0.3 mM) on the outside of the on-cell giant pipette. Figure 9a shows line scans in an axis through the pipette tip before and 30 s after application of carbachol. As already noted, the cells usually underwent profuse blebbing within 10–20 s of applying carbachol, and this causes the membrane boundary to move both within and outside of the pipette (cell images in Fig. 9a). The fact that membrane blebbing occurs rapidly within the pipette, when carbachol is applied outside the pipette, documents that this complex cellular response to PLC activation and PIP_2 depletion (Sheetz et al., 2006) propagates with little or no delay across the pipette boundary. As further illustrated by these line scans, peak fluorescence at the edge of cells often did not increase in spite of the fact that fluorescence in central regions of the cell decreased. This complexity may be related in part to the membrane blebbing and in part to the high concentration of cytoplasmic C1 domains achieved by overexpression. In any case, it was not possible to determine that any DAG gradients occurred in the cell surface using this approach.

As shown in Figure 9b, repeated activation of M1 receptors caused repeated strong reductions of C1 domain in the cytoplasm of the cell as well as in the cytoplasm drawn into the pipette. From normalized results of these specific experiments and five similar ones, we report that the largest differences in time courses between signals in the bulk of the cytoplasm and in the pipette tip were on the order of 1.5 s. This is not unexpected since the diffusion distances from the center of the cell to the cell membrane are even larger than the distance from the pipette orifice to the cell membrane in the pipette tip. Thus, the lack of C1 domain gradients in these experiments simply documents that the C1 domain can diffuse within cells with a diffusion coefficient of at least 3 $\mu m^2/s$, as expected for free diffusion of small proteins (i.e., $\sim$10,000 kDa).

That DAG analogues rapidly cross the membrane bilayer and diffuse across cells without causing membrane blebbing is documented in Figure 10. In the experiment illustrated, 2 μM dioctanoylglycerol (DAG8) a DAG analog was perfused into the pipette tip 25 s after the start of imaging. The C1-GFP fluorescence signal was monitored in different areas of the cell, as indicated in Figure 10b. The fluorescence of the entire cytoplasm decreases with a time constant of less than 1 min when DAG8 is applied to a membrane area that is at most 1/40 of the total cell membrane. We note in this context the close similarity of these time courses to those expected for free phospholipid

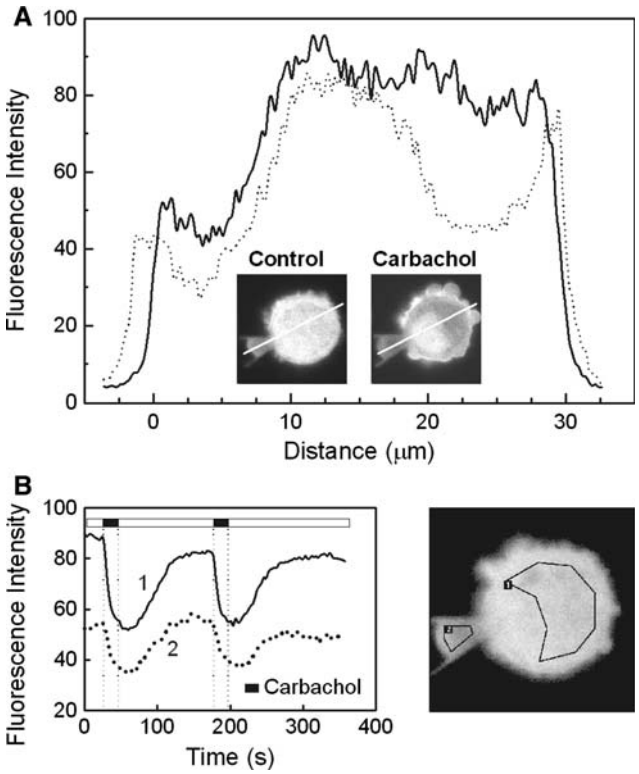

Fig. 9 BHK cell stably expressing hM1 receptors and transiently transfected with GFP-C1. The cell membrane outside the pipette was exposed to carbachol (0.3 mM) twice, as indicated by *solid bars* in **b**. **(a)** Line scans and cell images before and 30 s after exposure to carbachol. Each time the cell is exposed to carbachol, blebbing occurs over the entire cell, including plasma membrane not exposed to carbachol within the pipette. The blebbing is documented here as a shift of membrane position in the pipette (see line scans). **(b)** GFP-C1 domain fluorescence for the bulk of the cell cytoplasm (*1*, *solid line*) and for cytoplasm within the patch pipette tip (*2*, *dotted line*). The GFP-C1 domain responses are nearly identical in time course and recover within 1 min for the most part after removal of carbachol

diffusion in simple membrane bilayers, as illustrated in the Appendix for PIP_3 diffusion across the surface of a cell with similar dimensions. In summary, we have uncovered no evidence for restriction of PIP_2 or DAG8 diffusion in the cells employed in this study.

Discussion

We have characterized PIP_2 diffusion in the surface membranes of fibroblasts by two approaches. Using the FRAP method for PIP_2 and PC in the extracellular cell membrane monolayer and in membrane lawns, we obtained diffusion coefficients that are smaller than expected for simple membrane bilayers by a factor of 3–10. Using a completely different approach for the cytoplasmic monolayer, we expressed receptors that couple to PLC together with fluorescent lipid-binding domains to generate and visualize lipid gradients across entire cells, and we obtained no evidence that PIP_2 or DAG diffusion is restricted. We consider here the complexities, limitations and implications of these experiments.

Exogenous PIP_2 Diffusion

Exogenous phospholipids with fluorescent labels have been used extensively to analyze the lateral mobility of membrane lipids in a variety of cell types (Vaz et al., 1979; Jacobson, 1983; Almeida & Vax, 1995). Most probes form micelles that allow spontaneous incorporation of fluorescent monomers into cell membranes by a reaction that can rapidly exchange micelle probes with probes in the cell membrane (Flanagan et al., 1997; Elvington & Nichols, 2007; Pagano et al., 1981; Pagano & Huang, 1975). In our experience with pipette perfusion of cells via giant patch pipettes, several commonly used hydrophobic fluorescent membrane probes, and especially PIP_2, bind profusely throughout the cytoplasm and presumably on internal membranes (Fig. 1). These complications clearly preclude any simple use of these probes in FRAP experiments to analyze diffusion in the cytoplasmic membrane leaflet. It is not clear why our experience is different from that of others, in particular with atrial myocytes (Cho et al., 2005a). It will be important, therefore, to apply additional techniques to the cell types that have given highly conflicting results with the FRAP technique (Cho et al., 2006). We suspect that our use of large-diameter pipette tips facilitates phospholipid diffusion into and subsequently throughout the cytoplasm of cells. Even if large pools of fluorescent probes exist outside of the surface membrane, it may be possible to determine short-term diffusion coefficients in small membrane volumes with other techniques such as fluorescence correlation spectroscopy (Schwille & Haustein, 2007).

To enhance its solubility and reliable application, the PC used in the present study had a C6 side chain. Owing to the more hydrophilic nature of PIP_2, it could be incorporated efficiently into membrane lawns with C16 side chains. The diffusion coefficients determined for these two probes, in both membrane lawns and intact cells, were rather similar, suggesting that they encounter similar frictions. This is to some extent surprising as the longer NBD-labeled side chain probably loops back to the membrane surface (Chattopadhyay, 1990). The results appear to confirm that NBD-labeled phospholipids indeed imitate multiple behaviors of native lipids in membranes (Pagano & Sleight, 1985). Therefore, we see no clear reason to question the outcome that phospholipids in the outer monolayer of these fibroblasts diffuse 3–10 times slower than expected for simple bilayers. In fact, the on-cell outcomes are similar to outcomes described for neurons (Pucadyil &

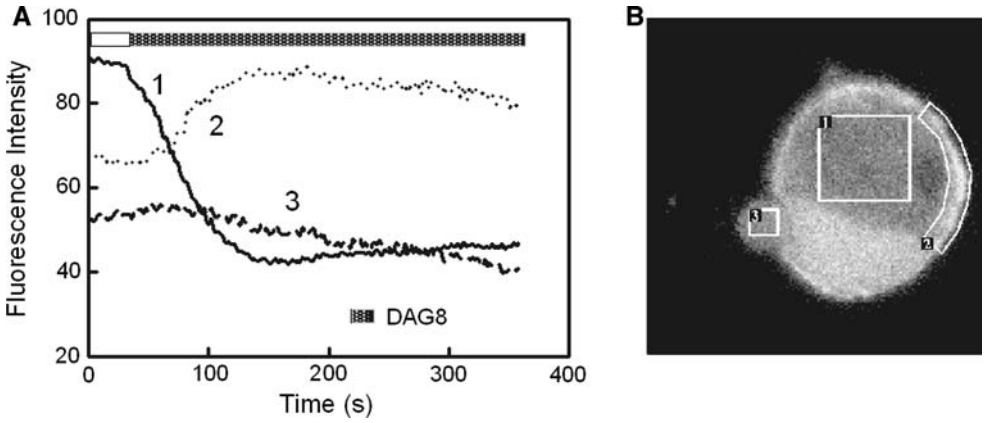

Fig. 10 Diffusion of short chain diacylglycerol (DAG8, 2 μM) throughout a BHK cell subsequent to its perfusion into an on-cell patch pipette. Perfusion is initiated at the twenty-fifth second, and the GFP-C1 domain moves to the cell membrane and out of the cytoplasm in the entire cell with an approximate time constant of 60 s. Result 1 (*solid line*) is the average fluorescence of the cytoplasm, 2 (*dotted line*) gives fluorescence of the membrane opposite the pipette tip and 3 (*dashed line*) gives fluorescence of cytoplasm drawn into the pipette tip. The fluorescence pattern gives no indication that DAG8 crosses through the cytoplasm, which would result in a characteristic C1 domain waveform. The time course of signals corresponds reasonably to those expected for free phospholipid diffusion laterally in a membrane, as expected from Figure 1

Chattopadhyay, 2006). Substantial accelerating effects of cholesterol removal suggest that the condensing function of cholesterol (Hung et al., 2007) in the outer monolayer may play a significant role in slowing phospholipid diffusion.

The major concern in membrane lawns is clearly the disposition of phospholipids with respect to inner and outer monolayers. In the simplest case, phospholipids are randomized between monolayers, and the diffusion coefficients obtained may be intermediate between real values in the outer and inner membrane leaflets. Regardless of the details, it is notable that we did not find slow components of PIP_2 (or PC) diffusion in this preparation, which might be caused by extensive lipid binding to membrane proteins and/or a fence function of the cytoskeleton. In so far as this membrane model maintains peripheral membrane proteins, which are potentially important determinants of PIP_2 diffusion, we find no evidence for any significant restriction.

Endogenous PIP_2 Diffusion

Fusions of the PLC-δ PH domain with GFP are presently widely used as a means to detect changes of PIP_2 in living cells. To our knowledge, this was the first attempt to determine a diffusion coefficient with these domains. There were two prerequisites, which appear to be met: first, it was possible to generate regional PIP_2 depletions in cells via overexpression of G_q-coupled receptors and, second, the PH domains bind and dissociate from PIP_2 fast enough to detect lipid gradients. The Tubby domains, which do not bind IP_3, overcome the specificity limitation of PH domains in binding both PIP_2 and IP_3. Even membrane blebbing occurs rapidly in areas where agonist has not been applied, suggesting that signaling lipids move rapidly in lateral directions. In Figures 6–8, PH domains respond within 6–10 s at distances of 6–10 μ from the sites where agonist is applied to cells. To explain the data set, we conclude that PIP_2 diffusion coefficients must be at least 1 and possibly 3 $\mu m^2/s$, and diffusion of DAG appears to occur at least as fast from the C1 domain signals obtained (Figs. 9, 10).

There are two significant limitations to our estimates of PIP_2 diffusion rates. First, Ca may be released in areas where PIP_2 is cleaved initially and, upon diffusion to neighboring membrane zones, promote PLC activation and PIP_2 cleavage. Free Ca in the micromolar range is known to promote activation of PLC by G-protein signaling (Horowitz et al., 2005). In the absence of G-protein activation, however (i.e., outside the region of agonist application), we are aware of no evidence that substantial PLC activities are stimulated by the free Ca concentrations achieved by Ca release in these cell types (0.3–2 μM [Luo et al., 2001]). Second, the continuous generation and degradation of PIP_2 by lipid kinases and phosphatases may complicate the experimental results. As described in Figure 6, we used simulations to address this complexity. From whole-cell experiments and experiments with application of carbachol outside the pipette (e.g., Fig. 7), we know that PH domains can be lost almost completely from the cell surface upon activation of receptors. However, when agonist is applied to a limited cell area, the nadir of signals corresponds to loss of only about 25% of the domains. The fact that domains continue to be lost from adjacent membrane requires that PIP_2 can diffuse rapidly across the pipette wall and that PIP_2 diffuses continuously

into the membrane within the pipette where PLC is activated. These processes evidently come to a steady state within about 25 s. To account for this, it is essential that PIP_2 turnover in the region not exposed to agonist takes place within this same time frame, presumably via simultaneous lipid phosphatase and kinase activities.

To conclude, we point out that Ca signals occur on a nanometer scale in cells because millions of Ca ions can diffuse through ion channels each second into a cytoplasm with very low free Ca (Carrera et al., 2007; Hinch, Greenstein & Winslow, 2006). For PIP_2, a robust physical basis for nanometer-scale gradients is not established. A sharp PIP_2 gradient, which can be visualized across the neck of phagosomes (Botelho et al., 2000; Scott et al., 2005), would appear to require a physical diffusion restriction, whereas extended gradients over several microns, e.g., along the membrane furrow that forms during cytokinesis (Emoto et al., 2005; Saul et al., 2004), do not require restrictions. Our data provide no evidence that bulk PIP_2 diffusion is restricted on the cytoplasmic side of cells employed in this study. Entirely new approaches seem required now to determine more definitely whether diffusion coefficients for small fractions of total PIP_2, e.g., in membrane buds in the process of endocytosis, might be radically lower.

Acknowledgements This work was supported by NIH-HL067942 and HL5132312 to D. W. H. We thank Mei-Jung Lin for outstanding technical assistance, Rene Bartz for advice about the membrane lawn preparation, Siyi Feng and Ping Dong for technical help and Vincenzo Lariccia for critical discussions.

Appendix

Simulations of PIP_3 and PIP_2 Diffusion

The most analyzed example of spatially organized phospholipid signaling is the PIP_3 gradient that develops from the leading to the trailing edge of migrating cells (Devreotes & Janetopoulos, 2003; Insall & Weiner, 2001). As underscored by simulations here, the existence of the PIP_3 gradients requires no restriction of lipid diffusion, and the time courses with which gradients develop are accounted for very well by phospholipid diffusion coefficients, as expected for simple bilayers with no restrictions. For the simulation illustrated in Figure 11, it is assumed that lipid kinases (PI3-kinases) are localized to 1% of total cell membrane at the left pole of the cell, while PIP_3 phosphatases (PTEN) are localized to 1% of the cell membrane at the right cell pole with enough activity to hydrolyze most of the cell's PIP_3 within 2 min. With a diffusion coefficient expected for simple phospholipid bilayers, 1–4 $\mu m^2/s$ (Jacobson, 1983), the average PIP_3 molecule requires a good minute to traverse the cell length (20 μm) from its site of synthesis to its site of degradation. Gradients develop with apparent time constants of 30–60 s when lipid kinase activity is increased in a stepwise fashion, and these times are consistent with experimental data and previous simulations (Ma et al., 2004).

As outlined in the "Introduction," it is proposed that PIP_2 depletion during PLC activation can occur on a nanometer scale so as to mediate signals from specific receptors to specific ion channels (Cho et al., 2005a, 2005b). Figure 12 illustrates the drastic extent to which lipid mobility would have to be restricted to explain such highly localized signals. Figure 12a presents simulation of a 1-μ-diameter disk of membrane with 50,000 PIP_2 molecules (i.e., about 1% of total phospholipid in the cytoplasmic leaflet), as expected for the plasma membrane of most mammalian cells (e.g., Nasuhoglu et al., 2002). A single PLC is assumed to exist at the center of the membrane disk. Its activity is assumed to be 1,000 s^{-1}, the maximal rate that we can project from biochemical studies (Smrcka & Sternweis, 1993). When the PLC is activated, PIP_2 is depleted uniformly across the membrane disk. Similarly, PIP_2 gradients remain negligible when the activity is simulated in an infinite sheet of membrane (*simulation not shown*).

In this same context, one may consider whether continuous metabolism of PIP_2 by phosphatases and lipid kinases might allow larger and/or more local gradients to

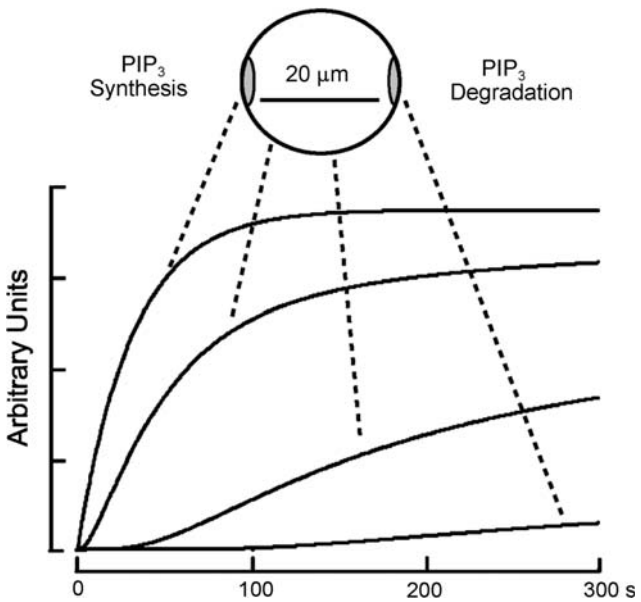

Fig. 11 Simulation of PIP_3 gradients in a cell assumed to be spherical and 20 μm in diameter with lipid kinases located to 1% of the cell area at one pole (*PIP_3 synthesis*) and lipid phosphatases located to 1% of cell area at the opposite pole (*PIP_3 degradation*). Degradation rate is 0.1/s within the degradation pole, and the diffusion coefficient is 2 $\mu m^2/s$. The cell contains initially no PIP_3, and PIP_3 synthesis is initiated at time 0

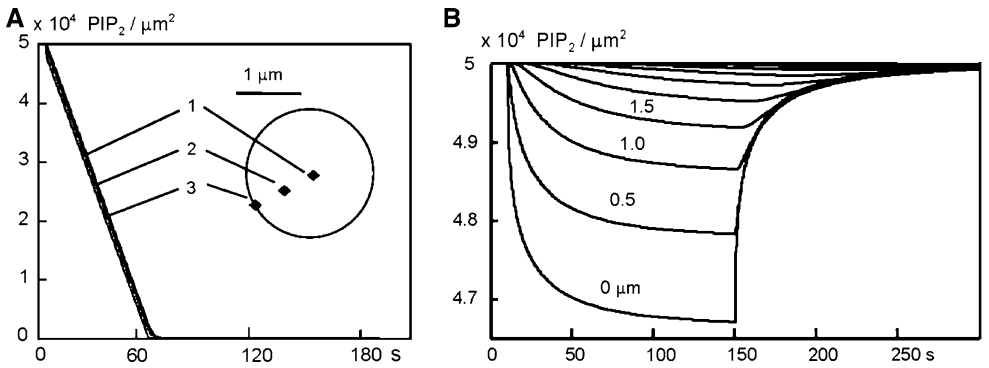

Fig. 12 Simulated PIP_2 gradients generated by a single PLC degrading PIP_2 at a rate of 1,000 s^{-1}. The PIP_2 density is assumed to be 50,000/μ^2 in steady state, equivalent to approximately 1% of the cytoplasmic monolayer; and the diffusion coefficient is 2 $\mu m^2/s$. **(a)** Disk model. The single PLC begins to cleave PIP_2 at the tenth second. PIP_2 densities remain nearly homogeneous as PIP_2 is cleaved from the disk. **(b)** Infinite sheet model. Activity of a single PLC is initiated at 10 s and terminated at 150 s in an infinite sheet of membrane. Everywhere within the sheet, PIP_2 is assumed to be simultaneously and homogeneously degraded at 0.03/s and synthesized at 1,500 molecules s^{-1} μm^{-2}. Results are given for the point of PIP_2 hydrolysis and for radii spaced at 0.5-μm intervals from the PLC activity. The approximately 6% depletion at the point of hydrolysis dissipates laterally with a space constant of 1 μm

develop with PLC activation. Figure 12b illustrates the PIP_2 gradients that are generated by the same punctate PLC activity in a membrane in which it is assumed that PIP_2 is generated and destroyed everywhere by lipid kinases and phosphatases so that the average PIP_2 lifetime is about 30 s. These assumptions are in fact required to reconstruct signals described subsequently for PH domains in intact cells. Activation of PLC with an activity of 1,000 s^{-1} generates a gradient with a length constant of about 1 μm with these assumptions and with a peak magnitude of 6% of the background PIP_2. As pointed out by Cho et al. (2005a), for significant PIP_2 signals to occur between neighboring proteins, lipid diffusion must be restricted more than 100-fold, probably 1,000-fold.

References

Aggeler J, Takemura R, Werb Z (1983) High-resolution three-dimensional views of membrane-associated clathrin and cytoskeleton in critical-point-dried macrophages. J Cell Biol 97:1452–1458

Almeida PFF, Vax WLC (1995) Lateral diffusion in membranes. In: Lipovsky R, Sackmann E (eds), Physics of biological systems: structure and dynamics of membranes. Elsevier, New York, pp 305–357

Botelho RJ, Teruel M, Dierckman R, Anderson R, Wells A, York JD, Meyer T, Grinstein S (2000) Localized biphasic changes in phosphatidylinositol-4,5-bisphosphate at sites of phagocytosis. J Cell Biol 151:1353–1368

Brown DA (2006) Lipid rafts, detergent-resistant membranes, and raft targeting signals. Physiology (Bethesda) 21:430–439

Brown DA, Hughes SA, Marsh SJ, Tinker A (2007) Regulation of M (Kv7.2/7.3) channels in neurons by PIP2 and products of PIP2 hydrolysis: significance for receptor-mediated inhibition. J Physiol 582:917–925

Bunce MW, Gonzales ML, Anderson RA (2006) Stress-ING out: phosphoinositides mediate the cellular stress response. Sci STKE 2006:e46

Carrera G, Gil A, Segura J, Soria B (2007) Software for simulating calcium-triggered exocytotic processes. Am J Physiol 292:C749–C755

Chattopadhyay A (1990) Chemistry and biology of *N*-(7-nitrobenz-2-oxa-1,3-diazol-4-yl)-labeled lipids: fluorescent probes of biological and model membranes. Chem Phys Lipids 53:1–15

Chen Y, Yang B, Jacobson K (2004) Transient confinement zones: a type of lipid raft? Lipids 39:1115–1119

Cho H, Kim YA, Ho WK (2006) Phosphate number and acyl chain length determine the subcellular location and lateral mobility of phosphoinositides. Mol Cells 22:97–103

Cho H, Kim YA, Yoon JY, Lee D, Kim JH, Lee SH, Ho WK (2005a) Low mobility of phosphatidylinositol 4,5-bisphosphate underlies receptor specificity of Gq-mediated ion channel regulation in atrial myocytes. Proc Natl Acad Sci USA 102:15241–15246

Cho H, Lee D, Lee SH, Ho WK (2005b) Receptor-induced depletion of phosphatidylinositol 4,5-bisphosphate inhibits inwardly rectifying K+ channels in a receptor-specific manner. Proc Natl Acad Sci USA 102:4643–4648

Collins A, Hilgemann DW (1993) A novel method for direct application of phospholipids to giant excised membrane patches in the study of sodium-calcium exchange and sodium channel currents. Pfluegers Arch 423:347–355

Devreotes P, Janetopoulos C (2003) Eukaryotic chemotaxis: distinctions between directional sensing and polarization. J Biol Chem 278:20445–20448

Di PG, DeCamilli P (2006) Phosphoinositides in cell regulation and membrane dynamics. Nature 443:651–657

Dictus WJ, van Zoelen EJ, Tetteroo PA, Tertoolen LG, de Laat SW, Bluemink JG (1984) Lateral mobility of plasma membrane lipids in *Xenopus* eggs: regional differences related to animal/vegetal polarity become extreme upon fertilization. Dev Biol 101:201–211

Dietrich C, Yang B, Fujiwara T, Kusumi A, Jacobson K (2002) Relationship of lipid rafts to transient confinement zones detected by single particle tracking. Biophys J 82:274–284

Ellenberg J, Siggia ED, Moreira JE, Smith CL, Presley JF, Worman HJ, Lippincott-Schwartz J (1997) Nuclear membrane dynamics and reassembly in living cells: targeting of an inner nuclear membrane protein in interphase and mitosis. J Cell Biol 138:1193–1206

Elson EL, Schlessinger J, Koppel DE, Axelrod D, Webb WW (1976) Measurement of lateral transport on cell surfaces. Prog Clin Biol Res 9:137–147

Elvington SM, Nichols JW (2007) Spontaneous, intervesicular transfer rates of fluorescent, acyl chain-labeled phosphatidylcholine analogs. Biochim Biophys Acta 1768:502–508

Emoto K, Inadome H, Kanaho Y, Narumiya S, Umeda M (2005) Local change in phospholipid composition at the cleavage furrow is essential for completion of cytokinesis. J Biol Chem 280:37901–37907

Flanagan LA, Cunningham CC, Chen J, Prestwich GD, Kosik KS, Janmey PA (1997) The structure of divalent cation-induced aggregates of PIP2 and their alteration by gelsolin and tau. Biophys J 73:1440–1447

Galla HJ, Hartmann W, Theilen U, Sackmann E (1979) On two-dimensional passive random walk in lipid bilayers and fluid pathways in biomembranes. J Membr Biol 48:215–236

Golan DE, Alecio MR, Veatch WR, Rando RR (1984) Lateral mobility of phospholipid and cholesterol in the human erythrocyte membrane: effects of protein–lipid interactions. Biochemistry 23:332–339

Greenberg ML, Axelrod D (1993) Anomalously slow mobility of fluorescent lipid probes in the plasma membrane of the yeast *Saccharomyces cerevisiae*. J Membr Biol 131:115–127

Hilgemann DW, Collins A (1992) Mechanism of cardiac Na^+-Ca^{2+} exchange current stimulation by MgATP: possible involvement of aminophospholipid translocase. J Physiol 454:59–82

Hilgemann DW, Feng S, Nasuhoglu C (2001) The complex and intriguing lives of PIP2 with ion channels and transporters. Sci STKE 2001:RE19

Hilgemann DW, Lu CC (1998) Giant membrane patches: improvements and applications. Methods Enzymol 293:267–280

Hinch R, Greenstein JL, Winslow RL (2006) Multi-scale models of local control of calcium induced calcium release. Prog Biophys Mol Biol 90:136–150

Horowitz LF, Hirdes W, Suh BC, Hilgemann DW, Mackie K, Hille B (2005) Phospholipase C in living cells: activation, inhibition, Ca^{2+} requirement, and regulation of M current. J Gen Physiol 126:243–262

Hung WC, Lee MT, Chen FY, Huang HW (2007) The condensing effect of cholesterol in lipid bilayers. Biophys J 92:3960–3967

Hussain NK, Yamabhai M, Ramjaun AR, Guy AM, Baranes D, O′Bryan JP, Der CJ, Kay BK, McPherson PS (1999) Splice variants of intersectin are components of the endocytic machinery in neurons and nonneuronal cells. J Biol Chem 274:15671–15677

Ilangumaran S, Hoessli DC (1998) Effects of cholesterol depletion by cyclodextrin on the sphingolipid microdomains of the plasma membrane. Biochem J 335(Pt 2):433–440

Insall RH, Weiner OD (2001) PIP3, PIP2, and cell movement—similar messages, different meanings? Dev Cell 1:743–747

Jacobson K (1983) Lateral diffusion in membranes. Cell Motil 3:367–373

Jacobson K, Mouritsen OG, Anderson RG (2007) Lipid rafts: at a crossroad between cell biology and physics. Nat Cell Biol 9:7–14

Jafri MS, Keizer J (1995) On the roles of Ca^{2+} diffusion, Ca^{2+} buffers, and the endoplasmic reticulum in IP3-induced Ca^{2+} waves. Biophys J 69:2139–2153

Jenkins GM, Frohman MA (2005) Phospholipase D: a lipid centric review. Cell Mol Life Sci 62:2305–2316

Kahya N, Scherfeld D, Bacia K, Schwille P (2004) Lipid domain formation and dynamics in giant unilamellar vesicles explored by fluorescence correlation spectroscopy. J Struct Biol 147:77–89

Kirchhausen T, Boll W, van OA, Ehrlich M (2005) Single-molecule live-cell imaging of clathrin-based endocytosis. Biochem Soc Symp 72:71–76

Kusumi A, Nakada C, Ritchie K, Murase K, Suzuki K, Murakoshi H, Kasai RS, Kondo J, Fujiwara T (2005) Paradigm shift of the plasma membrane concept from the two-dimensional continuum fluid to the partitioned fluid: high-speed single-molecule tracking of membrane molecules. Annu Rev Biophys Biomol Struct 34:351–378

Ling K, Schill NJ, Wagoner MP, Sun Y, Anderson RA (2006) Movin′ on up: the role of PtdIns(4,5)P(2) in cell migration. Trends Cell Biol 16:276–284

Liu Y, Casey L, Pike LJ (1998) Compartmentalization of phosphatidylinositol 4,5-bisphosphate in low-density membrane domains in the absence of caveolin. Biochem Biophys Res Commun 245:684–690

Luo D, Broad LM, Bird GS, Putney JW Jr (2001) Signaling pathways underlying muscarinic receptor-induced $[Ca^{2+}]_i$ oscillations in HEK293 cells. J Biol Chem 276:5613–5621

Ma L, Janetopoulos C, Yang L, Devreotes PN, Iglesias PA (2004) Two complementary, local excitation, global inhibition mechanisms acting in parallel can explain the chemoattractant-induced regulation of PI(3,4,5)P3 response in dictyostelium cells. Biophys J 87:3764–3774

Milosevic I, Sorensen JB, Lang T, Krauss M, Nagy G, Haucke V, Jahn R, Neher E (2005) Plasmalemmal phosphatidylinositol-4,5-bisphosphate level regulates the releasable vesicle pool size in chromaffin cells. J Neurosci 25:2557–2565

Moore MS, Anderson RG (1989) Towards an in vitro system for studying clathrin-coated pit function. J Cell Sci Suppl 11:179–186

Nasuhoglu C, Feng S, Mao J, Yamamoto M, Yin HL, Earnest S, Barylko B, Albanesi JP, Hilgemann DW (2002) Nonradioactive analysis of phosphatidylinositides and other anionic phospholipids by anion-exchange high-performance liquid chromatography with suppressed conductivity detection. Anal Biochem 301:243–254

Oradd G, Westerman PW, Lindblom G (2005) Lateral diffusion coefficients of separate lipid species in a ternary raft-forming bilayer: a Pfg-NMR multinuclear study. Biophys J 89:315–320

Pagano RE, Huang L (1975) Interaction of phospholipid vesicles with cultured mammalian cells. II. Studies of mechanism. J Cell Biol 67:49–60

Pagano RE, Martin OC, Schroit AJ, Struck DK (1981) Formation of asymmetric phospholipid membranes via spontaneous transfer of fluorescent lipid analogues between vesicle populations. Biochemistry 20:4920–4927

Pagano RE, Sleight RG (1985) Defining lipid transport pathways in animal cells. Science 229:1051–1057

Parmryd I, Adler J, Patel R, Magee AI (2003) Imaging metabolism of phosphatidylinositol 4,5-bisphosphate in T-cell GM_1-enriched domains containing Ras proteins. Exp Cell Res 285:27–38

Press WH, Flannery BP, Teukolsky SA, Vetterlin WT (1986) Numerical Recipes: the art of scientific computing. Integration of ordinary differential equations, chap 15. Cambridge University Press, Cambridge, pp 560–588

Pucadyil TJ, Chattopadhyay A (2006) Effect of cholesterol on lateral diffusion of fluorescent lipid probes in native hippocampal membranes. Chem Phys Lipids 143:11–21

Raucher D, Stauffer T, Chen W, Shen K, Guo S, York JD, Sheetz MP, Meyer T (2000) Phosphatidylinositol 4,5-bisphosphate functions as a second messenger that regulates cytoskeleton-plasma membrane adhesion. Cell 100:221–228

Rhee SG (2001) Regulation of phosphoinositide-specific phospholipase C. Annu Rev Biochem 70:281–312

Rimon G, Meyerstein N, Henis YI (1984) Lateral mobility of phospholipids in the external and internal leaflets of normal and hereditary spherocytic human erythrocytes. Biochim Biophys Acta 775:283–290

Rizzoli SO, Richards DA, Betz WJ (2003) Monitoring synaptic vesicle recycling in frog motor nerve terminals with FM dyes. J Neurocytol 32:539–549

Rozelle AL, Machesky LM, Yamamoto M, Driessens MH, Insall RH, Roth MG, Luby-Phelps K, Marriott G, Hall A, Yin HL (2000). Phosphatidylinositol 4,5-bisphosphate induces actin-based movement of raft-enriched vesicles through WASP-Arp2/3. Curr Biol 10:311–320

Santagata S, Boggon TJ, Baird CL, Gomez CA, Zhao J, Shan WS, Myszka DG, Shapiro L (2001) G-protein signaling through tubby proteins. Science 292:2041–2050

Santarius M, Lee CH, Anderson RA (2006) Supervised membrane swimming: small G-protein lifeguards regulate PIPK signalling and monitor intracellular PtdIns(4,5)P2 pools. Biochem J 398:1–13

Saul D, Fabian L, Forer A, Brill JA (2004) Continuous phosphatidylinositol metabolism is required for cleavage of crane fly spermatocytes. J Cell Sci 117:3887–3896

Scandella CJ, Devaux P, McConnell HM (1972) Rapid lateral diffusion of phospholipids in rabbit sarcoplasmic reticulum. Proc Natl Acad Sci USA 69:2056–2060

Scherfeld D, Kahya N, Schwille P (2003) Lipid dynamics and domain formation in model membranes composed of ternary mixtures of unsaturated and saturated phosphatidylcholines and cholesterol. Biophys J 85:3758–3768

Schlessinger J, Koppel DE, Axelrod D, Jacobson K, Webb WW, Elson EL (1976) Lateral transport on cell membranes: mobility of concanavalin A receptors on myoblasts. Proc Natl Acad Sci USA 73:2409–2413

Schlessinger J, Axelrod D, Koppel DE, Webb WW, Elson EL (1977) Lateral transport of a lipid probe and labeled proteins on a cell membrane. Science 195:307–309

Schuck S, Simons K (2004) Polarized sorting in epithelial cells: raft clustering and the biogenesis of the apical membrane. J Cell Sci 117:5955–5964

Schwille P, Haustein E (2007) Fluorescence correlation spectroscopy: an introduction to its concepts and applications. http://www.biophysics.org/education/schwille.pdf

Scott CC, Dobson W, Botelho RJ, Coady-Osberg N, Chavrier P, Knecht DA, Heath C, Stahl P, Grinstein S (2005) Phosphatidylinositol-4,5-bisphosphate hydrolysis directs actin remodeling during phagocytosis. J Cell Biol 169:139–149

Selyanko AA, Hadley JK, Wood IC, Abogadie FC, Jentsch TJ, Brown DA (2000) Inhibition of KCNQ1-4 potassium channels expressed in mammalian cells via M1 muscarinic acetylcholine receptors. J Physiol 522(Pt 3):349–355

Shpetner HS, Herskovits JS, Vallee RB (1996) A binding site for SH3 domains targets dynamin to coated pits. J Biol Chem 271:13–16

Siggia ED, Lippincott-Schwartz J, Bekiranov S (2000) Diffusion in inhomogeneous media: theory and simulations applied to whole cell photobleach recovery. Biophys J 79:1761–1770

Singer SJ, Nicolson GL (1972) The fluid mosaic model of the structure of cell membranes. Science 175:720–731

Smrcka AV, Sternweis PC (1993) Regulation of purified subtypes of phosphatidylinositol-specific phospholipase C beta by G protein alpha and beta gamma subunits. J Biol Chem 268:9667–9674

Tetteroo PA, Bluemink JG, Dictus WJ, van Zoelen EJ, de Laat SW (1984) Lateral mobility of plasma membrane lipids in dividing *Xenopus* eggs. Dev Biol 104:210–218

Tocanne JF, Dupou-Cezanne L, Lopez A (1994) Lateral diffusion of lipids in model and natural membranes. Prog Lipid Res 33:203–237

Trauble H, Sackmann E (1972) Studies of the crystalline-liquid crystalline phase transition of lipid model membranes. 3. Structure of a steroid-lecithin system below and above the lipid-phase transition. J Am Chem Soc 94:4499–4510

van Meer G, Simons K (1986) The function of tight junctions in maintaining differences in lipid composition between the apical and the basolateral cell surface domains of MDCK cells. EMBO J 5:1455–1464

van Rheenen J, Achame EM, Janssen H, Calafat J, Jalink K (2005) PIP2 signaling in lipid domains: a critical re-evaluation. EMBO J 24:1664–1673

van Rheenen J, Jalink K (2002) Agonist-induced PIP_2 hydrolysis inhibits cortical actin dynamics: regulation at a global but not at a micrometer scale. Mol Biol Cell 13:3257–3267

Vaz WL, Jacobson K, Wu ES, Derzko Z (1979) Lateral mobility of an amphipathic apolipoprotein, ApoC-III, bound to phosphatidylcholine bilayers with and without cholesterol. Proc Natl Acad Sci USA 76:5645–5649

Wang YJ, Li WH, Wang J, Xu K, Dong P, Luo X, Yin HL (2004) Critical role of PIP5KIγ87 in InsP3-mediated Ca^{2+} signaling. J Cell Biol 167:1005–1010